Structure and Energetics of Iron Pentacarbonyl Formation at an Fe(100) Surface

Hansong Cheng,* David B. Reiser, Sheldon W. Dean, Jr., and Kenneth Baumert

Air Products and Chemicals, Inc., 7201 Hamilton Boulevard, Allentown, Pennsylvania 18195-1501

Received: July 18, 2001; In Final Form: October 16, 2001

Ab initio density functional theory is used to study an important chemical corrosion phenomenon: carbonyl formation on metal surfaces. Our initial focus is on the structural and energetic aspects of the iron pentacarbonyl formation on an Fe(100) surface. The surface is represented by a slab model, and the adsorption of CO molecules is described by an idealized model that allows the extraction of a metal atom from the surface while minimizing the lateral interactions. The carbonyl formation undergoes three major steps: the chemisorption of CO molecules to form surface carbonyl species, the desorption of the complex from the surface to form a transition state, and the evolution into the final product. Although the chemisorption of CO on Fe(100) is energetically favorable, the desorption of the surface carbonyl species is endothermic, but the required energy can be largely compensated by the adsorption energy. The present study demonstrated that the metal atoms can be depleted by the surrounding CO molecules to form iron pentacarbonyl.

1. Introduction

The formation of iron pentacarbonyl has been observed in many industrial processes, e.g., in the production of synthetic natural gas.[1,2] It occurs most frequently in CO handling equipment made of steels. CO reacts with the steel surfaces to form the carbonyl species, leading to the depletion of the metal from the equipment. The reaction can take place at ambient temperature. The compound is highly toxic, flammable, and when decomposed yields a finely divided iron powder that is pyrophoric in air. Iron carbonyl complexes have been a subject of intensive research because of their importance in organometallic chemistry.[3−7] Their structures and chemical bonding have been studied extensively in the literature and are in general well understood. In addition, a number of recent studies have dealt with CO chemisorption on Fe surfaces.[8,9] However, little effort has been made to address how the carbonyl species are actually formed upon CO adsorption on iron surfaces at an atomistic and molecular scale. A better understanding of the mechanism could be beneficial when considering the unpredictable formation of this compound in storage and shipment vessels and might even shed some light on a related phenomenon, CO stress corrosion cracking which occurs when water is present together with CO and steel stressed in tension.

We have recently utilized quantum-mechanical density functional theory to study several chemical corrosion phenomena.[10−13] We showed that the theoretical methods are capable of providing useful information on the nitriding and metal dusting mechanisms. In the present work, we use the periodic density functional theory to investigate the carbonyl formation on the Fe(100) surface by addressing the structural and energetic aspects of the processes that involve CO chemisorption and desorption of surface carbonyl species. The purpose of this work is to understand the elementary steps of the surface reactions and to gain insight into the reaction mechanisms. Steels are used in the CO handling equipment. Understanding the reactions on a clean Fe(100) surface is thus an important step toward understanding this phenomena on steels.

In practice, carbonyl formation on metal surfaces can undergo extremely complicated processes. To simplify the problem, we employ an idealized surface model represented by a slab that allows us to focus only on the iron pentacarbonyl formation while neglecting other reaction processes that might also take place simultaneously, such as CO dissociation to form surface carbides or oxides. The structures and energetics of various species involved in the carbonyl formation are obtained upon geometry optimization. Subsequently, the energies of the reaction processes are derived.

2. Surface Model

To minimize the number of surface atoms in the unit cell in the calculations, we examine the pentacarbonyl formation only on an Fe(100) surface. The surface is described by a slab of three atomic layers. We note that the chosen surface is relatively more compact than the higher indices of surfaces and thus is likely less reactive with the incoming CO molecules. Nevertheless, it allows us to use fewer surface atoms in the unit cell but at the same time provides a model with which we can estimate the upper bound of the reaction energies. Furthermore, the recent work by Nayak and co-workers on CO adsorption on the Fe(100) surface showed that using three atomic layers to describe the surface is largely sufficient.[8]

Many reactive processes can occur simultaneously upon CO adsorption, such as CO dissociation, steam carbon reaction, Boudouard reaction, etc. It is difficult to address all of the complicated processes at the same time. Here, we only focus on the formation of the carbonyl complex. In practice, it is likely that this process may undergo a sequence of reactive steps and occur at surface defect sites, terraces, or corners. However, modeling all of these sophisticated processes with the present method requires considerable computational resources. Our main intention here is to explore the upper bound of the reaction energetics required in the carbonyl formation processes. The Fe(100) surface serves this purpose reasonably well. We therefore concentrate on a highly idealized situation by considering the case that an iron atom to be extracted from the surface is surrounded by five CO molecules. This, of course, is

* To whom correspondence should be addressed.

10.1021/jp0155112 CCC: $20.00
Published on Web 11/21/2001

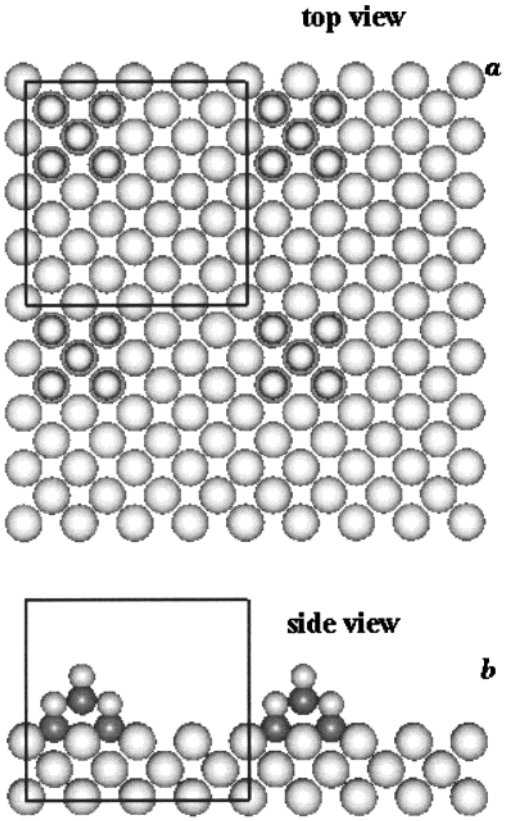

Figure 1. Unit cell as highlighted used in the calculations. Shown in a is the top view and in b is the side view. The large gray atom, Fe; the small gray atom, O; the black atom, C.

an unlikely scenario in practice. However, it allows us to estimate the maximum energy required to extract the metal atom from the surface to form the pentacarbonal species in the gas phase. To minimize the lateral interaction among the adsorbates, a sufficiently large unit cell is desirable. In this study, we select a unit cell of the slab that includes three layers of Fe atoms, each of which contains 4×4 primitive unit cells. On the top layer, four CO molecules reside at the hollow site to surround one iron atom and one CO is adsorbed at the atop mode of the metal atom. Overall, the unit cell contains 48 Fe atoms and 5 CO molecules. Figure 1 shows the selected unit cell used in our calculation. The unit cell parameters are $a = b = 11.466$ Å, $c = 14.412$ Å, $\alpha = \beta = \gamma = 90°$. Without counting the adsorbates, the vacuum between the slabs spans in the range of 11.530 Å, large enough to ensure no significant interaction between the slabs.

3. Computational Methods

For the slab calculation, we utilize the periodic ultrasoft pseudopotential density functional theory (DFT) with a plane wave basis set as implemented in the VASP code (Vienna Ab initio simulation package).[14−17] The Kohn−Sham equations are solved in a self-consistent manner under the generalized gradient approximation (GGA) as parametrized by Perdew and co-workers.[18] A spin-polarized computational scheme is employed to deal with the electronically open-shell system. Integrations of the Brillouin zone are done with only a single k point in light of the large cell parameters. The energy cutoff used in our calculation is 400 eV. Structural optimization is based on the conjugate gradient minimization scheme. The top two layers of the metal surface as well as the adsorbates are fully optimized, whereas the metal atoms of the bottom layer are not allowed to move.

TABLE 1: Calculated Structural Parameters and Chemisorption Energies for a Single CO Molecule on One Unit Cell of Fe(100)

	cluster model[a]		slab model (Wien)[a]		slab model (VASP)	
property	hollow	atop	hollow	atop	hollow	atop
C−O (pÅ)	1.32	1.19	1.30	1.17	1.31	1.18
Fe−C (Å)	1.90	1.82	1.98	1.82	1.97	1.79
Fe−O (Å)	2.23	3.01	2.10	3.00	2.15	2.97
θ (degree)[b]	54	0.00	54	0.00	49.8	0.00
ΔE (kcal/mol)	37.4	32.3			40.1	31.4

[a] Comparison is made between our slab model calculated with VASP and the cluster and slab models calculated with DMol3 and Wien97 by Nayak et al. [b] θ is the angle between the CO axis and the surface normal. The experimental value reported by Dwyer and co-workers[21] is $45 \pm 10°$.

For the molecular iron pentacarbonyl species, we use mostly the DFT-based computational package DMol,[3,19,20] which is capable of efficiently dealing with molecular systems. The spin-polarization calculation utilizes a double numerical basis set augmented with polarization functions. Full geometry optimization is performed without imposing symmetry constraint. The periodic DFT calculation by VASP for molecular systems requires a sufficiently large interstitial space between molecules to avoid direct intermolecular interactions and is thus computationally more demanding than the DFT calculation for a single molecule with DMol.[3] For purpose of comparison, we use VASP to perform a calculation for one molecule to calibrate the results obtained with DMol.[3]

4. Results and Discussions

4.1. CO Adsorption on the Fe(100) Surface. The optimized Fe(100) surface appears more closely packed than the bulk structure as expected. The interlayer distance is reduced by 0.066 Å to 1.367 Å.

We first examine the structure and properties of CO adsorbed at atop and hollow sites in the chosen unit cell. Nayak and co-workers[8] have recently performed DFT calculations with both cluster and slab models on this system and compared them with the experimental results reported earlier by Moon et al.[9] They found good agreement between their theoretical models and experiments. We note that their cluster model describes the low coverage adsorption, whereas their slab model represents the full monolayer where the lateral interaction between the adsorbates is significant. Here, we first focus on adsorption of only one CO at the atop and hollow sites using a much larger unit cell. The optimized geometric parameters and adsorption energies in our calculations compare very well with those by Nayak et al. and the available experiment, as shown in Table 1. At the atop mode, the adsorbing metal atom is raised slightly by about 0.22 Å, whereas at the hollow site, the nearby Fe atom is only marginally pushed up by about 0.11 Å.

We next calculate two CO molecules adsorbed at adjacent sites in the chosen unit cell. The results are shown in Table 2. For both molecules at the hollow sites, CO tilts away from the surface normal. The calculated average adsorption energy per molecule is about 42 kcal/mol. In particular, the two nearby Fe atoms between the adsorbates become much closer with a distance of 2.55 Å, 0.33 Å shorter than that prior to the adsorption, and slightly come above the surface by 0.05 Å. For adsorption with one CO on the atop mode and another on a nearby hollow site, the CO at the atop site tilts slightly toward the one at the hollow site. The adsorbing Fe atom is significantly lifted from the surface by the adsorbate by about 0.34 Å. The calculated average adsorption energy per CO molecule is 40.9 kcal/mol.

TABLE 2: Calculated Geometric Parameters and Chemisorption Energies for Two CO Molecules Adsorbed on the Selected Unit Cell of Fe(100) Surface

property	hollow + hollow	hollow + atop	
C−O (Å)	1.31	1.30	1.18
Fe−C (Å)	2.00	1.88	1.78
Fe−O (Å)	2.18	2.01	2.94
θ (degree)[a]	45.2	52.1	10.6
ΔE (kcal/mol)	84.1	81.7	

[a] θ is the angle between the CO axis and the surface normal.

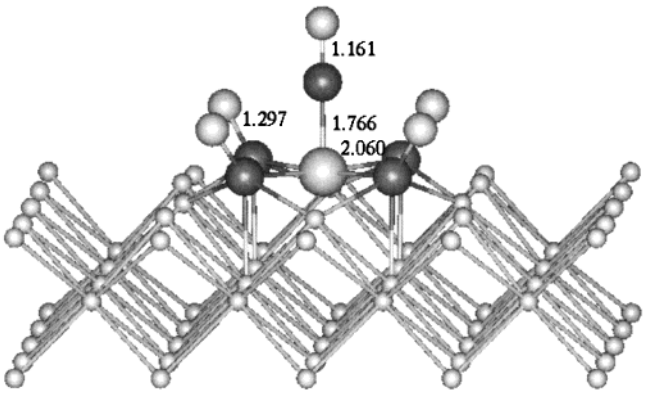

Figure 2. Optimized CO adsorption structure on Fe(100) surface. The surface $Fe(CO)_5$ species is highlighted with the CPK model.

The structure of Fe(100) changes significantly as more CO molecules are adsorbed on the surface. Figure 2 displays the optimized surface structure with five adsorbates. Some key geometric parameters are also displayed, and the surface iron pentacanbonyl species is highlighted with the CPK model. The metal atom surrounded by the CO molecules is visibly extracted from the surface. It is about 0.7 Å above the surface, much larger than the case where only one or two adsorbates are involved. Significant structural change also occurs to the neighboring metal atoms. The most noticeable one is the considerable deformation of the hollow sites to better accommodate the gas species: the four metal atoms of the hollow site are no longer coplanar; the distance between the central Fe atom and its adjacent atoms is shortened by 0.06 Å, and the Fe atom facing the center is pushed away by 0.14 Å; all of the metal atoms in the hollow site are raised vertically to a certain extent above the surface. The surrounding CO molecules lean away from the metal center with the angle from the surface normal approximately 38.9°, leading to the formation of iron pentacanbonyl. These CO molecules are highly activated by the metal atoms at the hollow site with significant bond elongation of 0.16 Å compared with the gas-phase value. The C−O bond stretch is further assisted by pulling over the O atom by the Fe atom at the corner opposite to the central Fe atom with an Fe−O distance of 2.057 Å. The carbon atoms reside about 0.74 Å above the surface. The capping CO molecule adsorbed at the on-top mode is much less activated, with bond elongation of 0.04 Å. The bond stretch can be readily understood on the basis of the electronic structure as will be elucidated later.

Upon the separation of the carbonyl species from the metal surface, the system first undergoes a metastable state with the carbonyl complex of C_{4v} symmetry. Vibrational mode analysis yields only one imaginary frequency (47i cm^{-1}), which corresponds to the normal mode that points to the formation of a trigonal bipyramid structure with a D_{3h} symmetry. The D_{3h} geometry of $Fe(CO)_5$ is known to be the ground-state structure.[22]

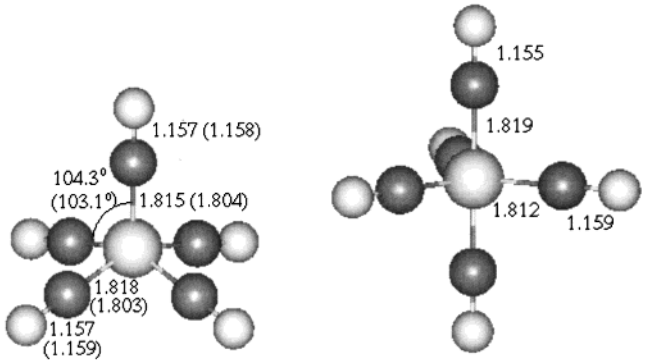

Figure 3. Optimized gas-phase $Fe(CO)_5$ species with (a) C_{4v} symmetry and (b) D_{3h} symmetry. The bond parameters in the parenthesis are obtained with VASP and the rest are calculated with DMol[3].

TABLE 3: Calculated Geometric Parameters of $Fe(CO)_5$ with D_{3h} Symmetry[a]

	Fe−C(ax.)	Fe−C(eq.)	C−O(ax.)	C−O(eq.)
this work	1.819	1.812	1.155	1.159
LDA[b]	1.769	1.789	1.145	1.149
DZP BP86[c]	1.805	1.805	1.167	1.170
DZP B3LYP[c]	1.823	1.816	1.152	1.156
expt.[d]	1.811	1.803	1.117	1.133
expt.[e]	1.807	1.827	1.152	1.152

[a] Comparison between the present calculation and the theoretical/experimental results reported in the literature is made. [b] Reference 7. [c] Reference 5. [d] Reference 4. [e] Reference 3.

The fully optimized geometries are shown in Figure 3. The C_{4v} structure, shown in Figure 3a, was obtained by using both DMol[3] and VASP. The calculated geometric parameters are in excellent agreement with each other. Note in particular that the capping CO molecule at the top of the pyramid pushes down the four CO molecules that form the square considerably. The transition state structure is only slightly higher in energy than the final product. Previous studies have described the interchange between the C_{4v} and D_{3h} structures with the Berry pseudorotation mechanism.[23,24] NMR studies suggested that the trigonal bipyramid geometry should be less than 1 kcal/mol lower in energy than the square pyramid structure.[25] Semiempirical calculations by Blyholder and Springs indicate that there is no energy barrier for the ligand interchange between axial and equatorial positions.[23] Our results are entirely consistent with their findings. In particular, the D_{3h} structure has been widely studied both experimentally and theoretically.[3−7] Table 3 lists the detailed comparison of the structural parameters.

The abstraction of the metal atom by CO molecules creates a vacancy on the surface. The optimized surface structure barely exhibits any appreciable geometric changes. The vacancy expands only slightly as the metal atoms at the edges tend to lean away from the vacancy to be more closely bound to other atoms. As a result, the Fe−Fe bond distance near the vacancy is reduced by 0.052 Å.

4.2. Energetics. In the current model system, the $Fe(CO)_5$ formation process is represented by the following three steps:

1. CO adsorption on Fe surface to form surface iron pentacarbonyl species

$$Fe(s) + 5CO(g) \rightarrow Fe{-}5CO(s)$$

where s and g stand for surface and gas phase, respectively. Fe(s) is the selected unit cell of Fe slab, and Fe−5CO(s) represents the cell with five CO molecules adsorbed in the fashion shown in Figure 2.

TABLE 4: Calculated Reaction Energies

reaction process	ΔE (kcal/mol)
Fe(s) + 5CO(g) → Fe-5CO(s)	−187.6
Fe-5CO(s) → Fe(s, vacancy) + $Fe(CO)_5$(g, C_{4v})	88.9
$Fe(CO)_5(C_{4v}) \rightarrow Fe(CO)_5(D_{3h})$	−0.9

2. The abstraction of surface $Fe(CO)_5$ into the gas phase to form a metastable structure of iron pentacarbonyl with a C_{4v} symmetry, creating a vacancy per unit cell on the surface

$$Fe-5CO(s) \rightarrow Fe(s, \text{vacancy}) + Fe(CO)_5(g, C_{4v})$$

where Fe(s, vacancy) is the selected unit cell of the Fe slab with one metal atom being extracted.

3. The evolution of the gas-phase $Fe(CO)_5$ from the metastable structure to the final product

$$Fe(CO)_5(g, C_{4v}) \rightarrow Fe(CO)_5(g, D_{3h})$$

The reaction energies are calculated in the following fashion. For reaction 1, it is defined as

$$\Delta E = E_{Fe-5CO(s)} - E_{Fe(s)} - 5E_{CO(g)}$$

where $E_{Fe-5CO(s)}$, $E_{Fe(s)}$, and $E_{CO(g)}$ are the electronic energies of the adsorbed structure, the selected unit cell of iron slab, and the gas-phase CO molecule, respectively. For reaction 2, the reaction energy is the energy required to desorb the iron pentacarbonyl species from the selected unit cell of the adsorbed Fe slab. The desorption yields a gas-phase $Fe(CO)_5$ complex with a C_{4v} symmetry and creates a vacancy on the unit cell of the Fe slab. The energies of each of the terms are obtained from their respective optimized structures. Finally, the reaction energy for reaction 3 is derived from the molecular calculation of the gas-phase $Fe(CO)_5$ complex with different symmetries.

The calculated reaction energies are shown in Table 4. It is seen that CO adsorption at the Fe(100) surface is extremely favorable with an average adsorption energy per CO of 37.5 kcal/mol. The central Fe atom is forced to partially come out of the surface, which allows further penetration of the CO molecules into the surface. The strong tendency of the surface $Fe(CO)_5$ formation is remarkable particularly in light of the supposedly less reactive (100) surface.

The calculated adsorption structure and energetics seem to suggest a "digging" mechanism for the $Fe(CO)_5$ formation: the CO molecules are initially adsorbed at the hollow site, push the surrounded metal atom which comes out of the surface, and then deepen their roots by forming strong bonding with the surface atoms. The structural optimization shows this is an energetically downhill process.

The calculated reaction energy for step *2* indicates that the desorption of the surface $Fe(CO)_5$ species is very endothermic, as expected. Carbonyl desorption remains an energetically uphill process until it reaches the transition state, at which the $Fe(CO)_5$ species forms a square-pyramid structure and is completely separated from the surface. The carbonyl species must overcome a stiff activation barrier before evolving into a stable trigonal bipyramid structure. However, the energy required is easily off set by the extremely exothermic adsorption energy. The activation barrier likely represents the upper bound of the energy required to form iron pentacarbonyl for the following reasons. First, the present study deals with a perfectly aligned and close-packed Fe surface, which is much less reactive than surfaces with terraces, defects, or sharp edges. Second, the calculation yields an activation energy to form a gas-phase carbonyl species. In practice, however, the carbonyl complexes remain on the surfaces as a liquid. The overall energy required to form these complexes is therefore expected to be much smaller. Nevertheless, the information about the upper bound activation energy is still useful for us to understand the corrosion process.

In conclusion, we find that the overall processes of iron pentacarbonyl formation are energetically favorable. We must point out that these processes represent only one of the plausible reaction pathways, as indicated by the calculated reaction energies. However, it is possible that the $Fe(CO)_5$ formation may undergo more complicated processes, particularly in the

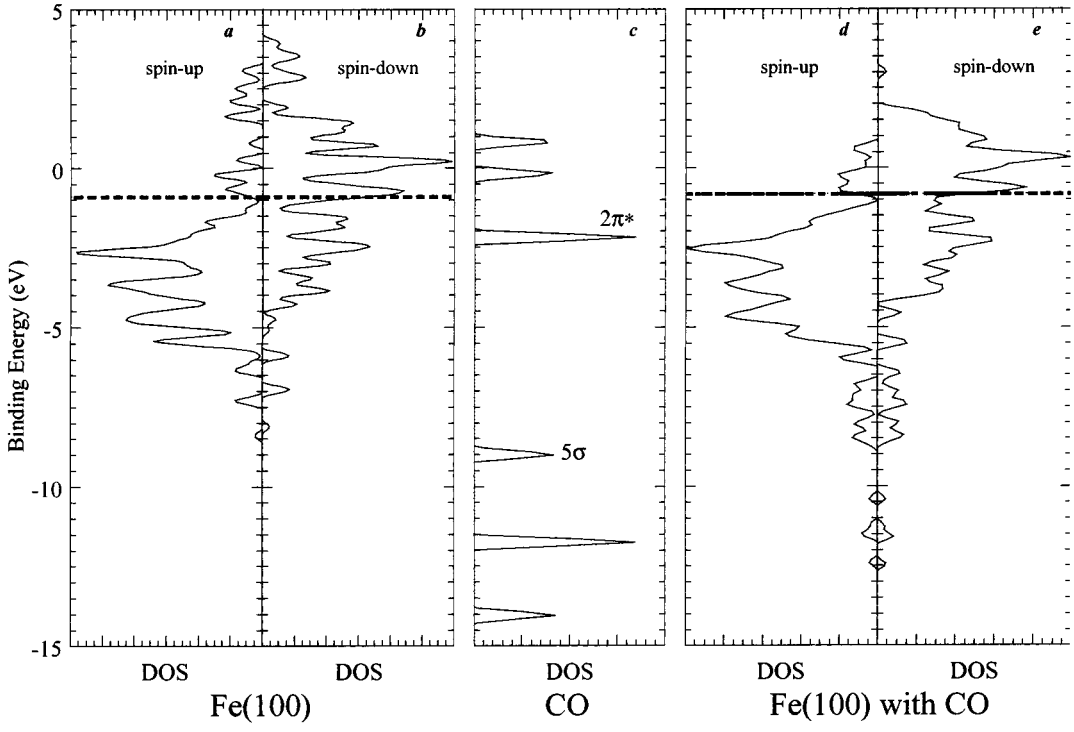

Figure 4. Calculated DOS spectra for Fe(100) (a and b), CO (c), and Fe(100) with five CO molecules adsorbed (d and e).

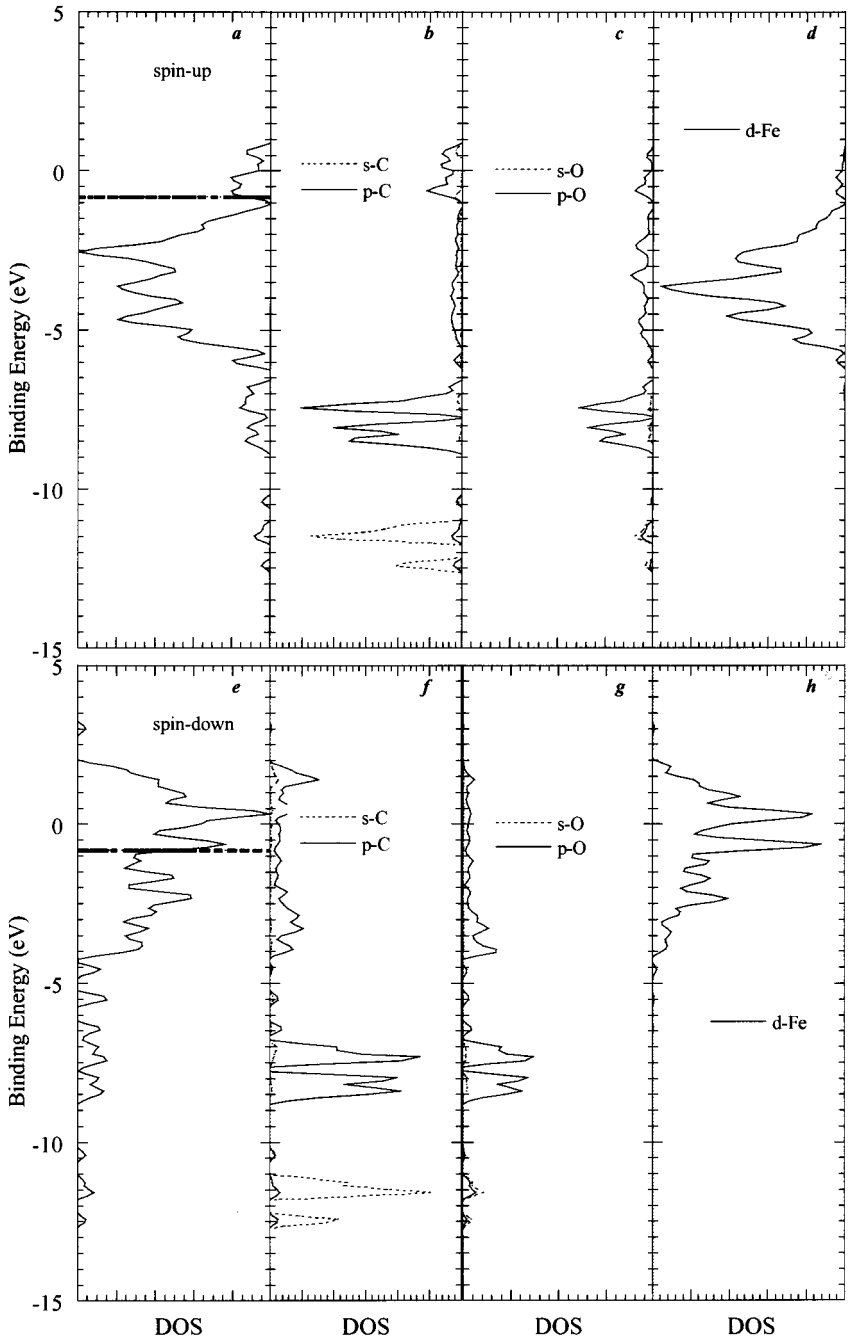

Figure 5. Projected DOS spectra. a and e are the total DOS of Fe(100) with five adsorbed CO molecules. The rest are projected orbital contributions from the atoms involved.

case of high density of CO adsorbates. The present model study serves the purpose of providing useful information on the metal depletion process resulting from the formation of iron pentacarbonyl.

4.3. Electronic Structure and Density States. There has been a vast amount of literature describing the nature of the interaction between CO and transition metals.[26] It can be briefly summarized as follows: the occupied 5σ orbital of CO, which is slightly antibonding, can readily overlap with the unoccupied d_{z^2} and 4s orbitals of the transition metal atoms with electron donation; the unoccupied 2π orbitals of CO are also capable of overlapping with the occupied d_{xz} and d_{yz} orbitals of metal atoms with electron back-donation. The back-bonding is more pronounced at the hollow sites, where the CO molecule is interacting with all of the neighboring metal atoms. This results in considerable bond stretch.

The electronic structure of the system can be described with the calculated electronic density of states (DOS). The DOS spectrum is also sensitive to the surface structural changes. Figure 4 displays the calculated DOS spectra of the Fe(100) surface, CO, and the Fe(100) with CO molecules adsorbed. The calculated Fermi levels are also labeled in the figures. For the Fe(100) surface, the energy bands right below the Fermi level are dominantly contributed to by the d orbitals. The occupied 5σ orbital of CO is well below these d bands, leading to a weak band overlap between 5σ of CO and d bands of Fe(100) surface. However, the empty $2\pi^*$ orbital of CO is about 2 eV lower than the Fermi level, allowing the CO molecules to accept electrons from the metal atoms. The antibonding nature of the $2\pi^*$ orbital of CO thus results in significant bond stretch in CO. Upon CO adsorption, the lower energy bands underneath the d bands of Fe reflect the electronic structural change of the adsorbates.

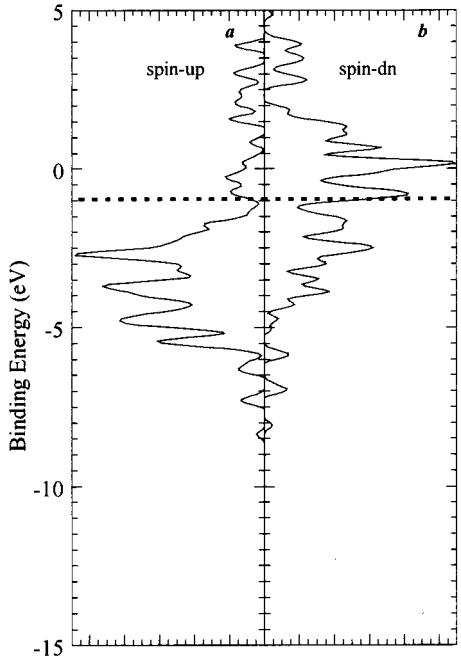

Figure 6. DOS spectra of Fe(100) with one vacancy per unit cell.

Figure 5 displays the calculated projected DOS spectra for the Fe(100) surface with adsorbates. It is clear that indeed the d bands of Fe dominate the energy bands near the Fermi level. A slight upward shift of the 5σ band and significant downward shift of the $2\pi^*$ band of CO are also observed. The band shift is the consequence of orbital overlapping: the weak $5\sigma-3d$ overlap results in slight electron flow from CO to the surface, which thus lifts the 5σ band to a higher level slightly; the strong $2\pi^*-3d$ overlap, however, gives rise to considerable electron back donation from Fe to CO, which lowers the $2\pi^*$ band significantly.

Finally, Figure 6 shows the calculated DOS spectrum of the Fe(100) surface with vacancies. Compared with the clean surface shown in Figure 3, the result suggests that the electronic band structure of the surface rarely changes upon the metal depletion by the CO molecules. This is consistent with the small geometric changes of the surface with vacancies.

5. Summary

Iron pentacarbonyl formation is a catastrophic corrosion process observed in many important industrial processes that involve CO molecules. The formation of this compound results in metal depletion from the surfaces of the equipment. Using quantum-mechanical density functional theory, we have explored the underlying possible reaction mechanisms by examining the structural and energetic properties of $Fe(CO)_5$ formation at the Fe(100) surface. We show that the CO chemisorption process is energetically very favorable to form the surface $Fe(CO)_5$ species. However, the desorption of $Fe(CO)_5$ from the surface is very endothermic. Nevertheless, the required desorption energy is more than compensated by the adsorption energy, leading to a thermochemically favorable process to form iron pentacarbonyl. Upon desorption from the metal surface, the carbonyl species first undergoes a metastable state with a square pyramid geometry and then further evolves into the final product with a trigonal bipyramid symmetry. The energy difference between the metastable structure and the final product is very small. The created vacancies on the surface due to the metal depletion do not result in significant surface structural changes.

The electronic structure analysis provides useful information on the nature of the surface reaction processes. The calculated DOS spectra suggest a strong back-bonding between the $2\pi^*$ orbital and the 3d bands of Fe atoms that gives rise to the chemisorption of CO. It is remarkable that even at the much less reactive Fe(100) surface the CO molecules are capable of reacting strongly with the surface by lifting the metal atom from the surface to form the $Fe(CO)_5$ species. Our results suggest a reaction mechanism in which the CO molecules dig into the hollow sites surrounding the metal atom and extract the atom out of the surface. Although the chemisorption process does not require an activation energy, the desorption of the surface carbonyl species is an energetically uphill process. The required desorption energy is compensated by the large chemisorption energy.

Finally, we emphasize that the present study deals with only a highly idealized model system for carbonyl formation, and as such, the CO molecules are placed only at the sites surrounding the metal atom to be depleted. In practice, other reaction events may also occur simultaneously. For example, the adsorbed CO may be further dissociated to form surface carbides or oxides. These processes will be addressed separately in our future work. The iron pentacarbonyl formation on a close-packed Fe(100) surface provides a useful model for us to gain insight into the upper bound energetics of the reaction processes.

Acknowledgment. H.C. would like to thank Prof. D. Sholl for useful discussions on the manuscript.

References and Notes

(1) Inouye, H.; DeVan, J. H. *J. Mater. Energy Syst.* **1979**, *1*, 52.
(2) Brynestad, J. *ORNL-TM-5499*; Oak Ridge National Laboratory, Oak Ridge, TN, 1976.
(3) Beagley, B.; Schmidling, D. G. *J. Mol. Struct.* **1974**, *22*, 466.
(4) Braga, D.; Grepioni, F.; Orpen, A. G. *Organometallics* **1993**, *12*, 1481.
(5) Jang, J. H.; Lee, J. G.; Lee, H.; Xie, Y.; Schaefer, H. F., III. *J. Phys. Chem. A* **1998**, *102*, 5298.
(6) Ehlers, A. W.; Frenking, G. *Organometallics* **1995**, *14*, 423.
(7) Li, J.; Schreckenbach, G.; Ziegler, T. *J. Am. Chem. Soc.* **1995**, *117*, 486.
(8) Nayak, S. K.; Nooijen, M.; Bernasek, S. L.; Blaha, P. *J. Phys. Chem. B* **2001**, *105*, 164.
(9) Moon, D. W.; Cameron, S.; Zaera, F.; Eberhardt, W.; Carr, R.; Bernasek, S. L.; Gland, J. L.; Dwyer, D. J. *Surf. Sci.* **1987**, *180*, L123.
(10) Cheng, H.; Reiser, D. B.; Mathias, P. M.; Baumert, K.; Dean, S. W., Jr. *J. Phys. Chem.* **1995**, *99*, 3715.
(11) Cheng, H.; Reiser, D. B.; Mathias, P. M.; Baumert, K.; Dean, S. W., Jr. *J. Phys. Chem.* **1996**, *100*, 9800.
(12) Cheng, H.; Reiser, D. B.; Dean, S. W., Jr. *AIChE J.* **1998**, *44*, 188.
(13) Cheng, H.; Reiser, D. B.; Dean, S. W., Jr. *Catal. Today* **1999**, *50*, 579.
(14) Kresse, G.; Hafner, J. *Phys. Rev. B* **1993**, *47*, 558.
(15) Kresse, G.; Hafner, J. *Phys. Rev. B* **1993**, *48*, 13115.
(16) Kresse, G.; Furthmüller, J. *J. Comput. Mater. Sci.* **1996**, *6*, 15.
(17) Kresse, G.; Furthmüller, J. *Phys. Rev. B* **1996**, *55*, 11169.
(18) Perdew, J. P.; Wang, Y. *Phys. Rev. B* **1992**, *45*, 13244.
(19) Delley, B. *J. Chem. Phys.* **1990**, *92*, 508.
(20) *DMol*^{3}, version 4.2; Molecular Simulations, Inc.: San Diego, CA, 1999.
(21) Dwyer, D. J.; Rausenberger, B.; Cameron, S. D.; Lu, J. P.; Bernasek, S. L.; Fischer, D. A.; Parker, D. H.; Gland, J. L. *Surf. Sci.* **1989**, *224*, 375.
(22) Cotton, F. A.; Wilkinson, G. *Advanced Inorganic Chemistry*; John Wiley & Son: New York, 1972.
(23) Blyholder, G.; Springs, J. *Inorg. Chem.* **1985**, *24*, 224.
(24) DiCarlo, E. N. *J. Am. Chem. Soc.* **1979**, *102*, 2205.
(25) Spiess, H. W.; Grosescu, R.; Haeberlen, U. *Chem. Phys.* **1974**, *6*, 226.
(26) van Santen, R. A.; Neurock, M. *Catal. Rev.—Sci. Eng.* **1995**, *37*, 557.